Characterization and Calibration Challenges of an K-Band Large-Scale Active Phased-Array Antenna with a Modular Architecture

Naimeh Ghaffarian[#1], Wael A. Wahab [#], Amir Raeesi [#], Ehsan Alian Aminabad [#], Ardeshir Palizban [#], Ahmad Ehsandar [#], Milad Khaki [#], Mohammad-Reza Nezhad-Ahmadi [#], Safieddin Safavi-Naeini [#]

[#]Centre for Intelligent Antenna and Radio Systems (CIARS), University of Waterloo, Canada

[1]n2ghafar@uwaterloo.ca

***Abstract*— In this paper, a comprehensive characterization and calibration of a K-band large scale active phased-array antenna (APAA) that consists of 1024 (32×32) radiating elements based on a modular architecture is presented. RF-channels are fully characterized inside the APAA environment using a planar near-field probe setup. A very accurate and efficient calibration technique is suggested and verified successfully over a wide range of scan angles (0 to 70 degree) and wide frequency band of 18-21 GHz.**

***Keywords*— active phased-array antenna, calibration, characterization, search algorithm, MMIC, modular architecture.**

I. Introduction

K/Ka-band High Throughput Satellite (HTS) communication system is identified as the future architecture to deliver broadband internet service, especially for remote areas coverage[1], [2]. Therefore, ongoing extensive efforts by researchers in industry and academia are aimed at developing a compact, low-profile, and cost-effective antenna solutions for K/Ka-band mobile Satellite Communication (SATCOM). Among different emerging technologies, active APAA systems can satisfy most of these requirements in emerging LEO satellite constellations as the main beam is steered electronically enabling higher speed, low latency, broadband, and high data rate in transmit and receive modes [3].

In mobile SATCOM applications, the antenna should be able to scan its beam toward the right satellite. Therefore, each radiating element is equipped with beam control devices such as phase shifter and Variable Gain Amplifier (VGA). Modular architecture is considered to be an effective and preferred approach in implementing large scale (high gain) APAA [4] as design complexity, PCB fabrication errors, and costs are minimized. In this architecture, the APAA system is made of a large number of identical subarray modules (building blocks). Therefore, it facilitates the implementation of APAA with any size without re-designing the modules, and depending on the SATCOM application requirements, only the backplane RF-feeding (combing or distributing) network should be customized.

Using this modular technology a large phased-array antenna with 1024 elements consisting of 64 identical sub-array modules is designed and fabricated for the first time in K-band (as shown in Fig. 1). For HTS applications precise beam scanning with beam pointing accuracy of ±0.1 degree and low cross polarization as well as compliance with radiation mask specifications are required. Therefore, precise calibration and characterization become critical challenging issues. Phase and amplitude unbalances of the radiating antenna elements are caused by different factors, such as embedded element pattern differences, gain and phase offsets of the RF electronics, temperature variations over the aperture, quantization of amplitude and phase settings and dissimilarity of internal connections. Among these factors, dissimilarities due to manually mounted modules-backplane connection is the most significant one.

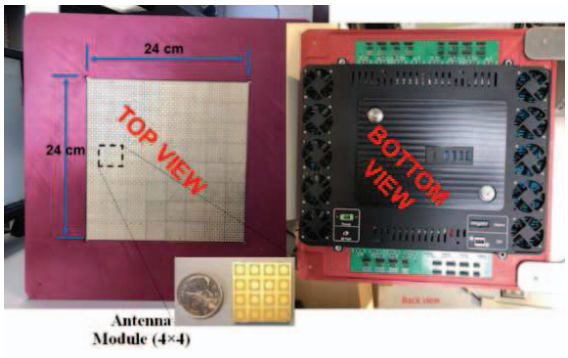

Fig. 1. 20 GHz 1024(32×32) APAA, top view (left) and bottom view (right).

Using low cost assembly technology will inevitably result in some degree of misalignment and disorientation. As a consequence, the modularity and cost effective fabrication processes require comprehensive calibration.

In this paper, an external calibration (factory calibration) technique based on near field measurements is employed to estimate the initial phase and magnitude unbalances among the elements, and to compensate for these errors. One of the key issues is that the elements behaviours in array environment are different from those in isolation, and which also depend on their location. Furthermore, other issues such as large number of elements (1024 element), wide frequency band and inter-dependence of phase and amplitude of each channel, increase the complexity and processing time of the calibration procedure. These challenges will be discussed in more details in Sections II and III which present the frequency

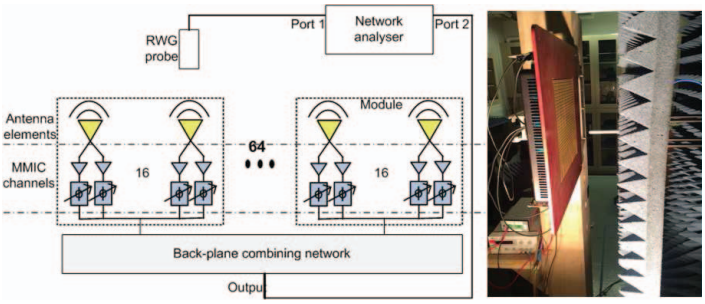

Fig. 2. Measurment and calibration setup.

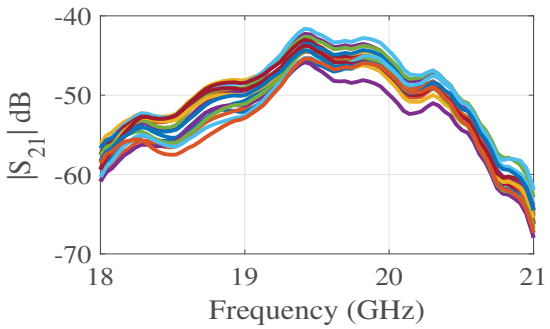

Fig. 3. Amplitude of S21 for 16 individually excited elements inside a module located at the centre of the phased-array.

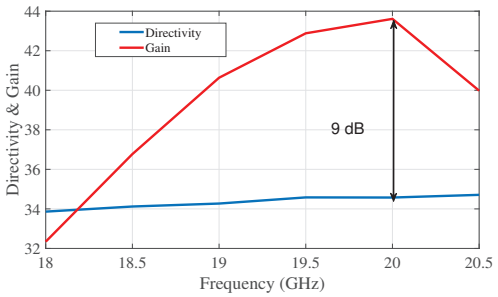

Fig. 4. Gain and directivity of 32×32 element array over frequency.

and MMIC channel characterizations respectively. Considering these challenges, a precise and efficient calibration method is developed. The details of this method along with the measurement results are presented in Section IV.

II. Frequency Characterization

Fig. 2 shows the calibration system configuration for receiver array. The APAA under test consists of 64 modules. Each module contains a 4×4 sub-array of dual-polarized, high efficiency, and broadband elements. The 4×4 subarray module incorporates passive feed circuits and four beam-forming MMICs, each with eight RF channels to control the phase, amplitude and polarization of each antenna element independently. A four way power combiner is used to sum the output signals of all MMIC chips of the module into a single output. A customized back-plane combining network[3] is used to combine the output signals of all modules (see Fig. 2).

To investigate the frequency response of the system a near field scanner system with standard rectangular waveguide probes was used. The near-field probe is periodically placed in front of each individually excited antenna element while other elements are deactivated. The scattering parameter (S21) between the input port of the near-field system and output port of the phased-array antenna (see Fig. 2) is then measured over the frequency range of $18 - 21$ GHz. Fig. 3 shows the measured S21 for all elements within a module at the centre of the phased array. In this figure, all the elements are excited individually with the same phase shifter and VGA settings with the average MMIC gain of $\sim 9.5dB$. For each element, Fig. 3 shows the total frequency response of all components including patch antenna, MMIC channel, and backplane feeding network. In addition the free space path loss between the antenna and probe and the gain of the probe are also included in the S21 measurements.

Fig. 3 shows that although the amplitude offsets exist between different channels, the amounts of these offsets do not change significantly over the operational range of frequencies. Therefore, it is not required to calibrate the system over the entire frequency bandwidth.

Fig. 4 shows the measured gain and directivity of the array at broadside versus frequency. In this figure the antenna is calibrated at 19.5 GHz. However, the same calibrated settings are used for all frequencies within the band. As shown in this figure the directivity variation over the frequency is negligible. However, the gain frequency response of the whole array follows the frequency response of the entire channel (MMIC+feed circuit+antenna) for each element (Fig. 3). The difference between the gain and directivity equals the average active gain of the MMIC channels in the system minus the loss of passive components including loss of antennas, combiners, transitions, and back-plane combining structures.

III. MMIC Channel Characterization

The RF performance specifications of MMIC channels are commonly provided for individual MMICs on the evaluation board (eval-board). However, accurate system modelling and performance assessment require measurements of the active device characteristics in phased-array environment. The MMIC behaviour in phased-array environment is not the same as that on the eval-board. All characteristics such as the efficiency, the impedance matching, etc. are impacted by the environment. Therefore, the MMICs are characterized inside the array.

The results of MMIC characterization for one of the channels at 20 randomly chosen locations on the array are plotted in Fig. 4. Each MMIC channel has a 5 bit phase-shifter with 32 phase states and a 5 bit VGA with 32 amplitude states. Fig. 5a shows the variation of the measured S21 amplitude while VGA amplitude states change between state 1 (highest gain) to state 32 (lowest gain) and the phase shifter is at phase state 1. The measured amplitudes of each channel are normalized to the amplitude of the first amplitude state of that channel.

As depicted in Fig. 5a, not only are the relative VGA amplitude response of all MMIC chips not the same as the eval-board data, but they are also different from each other by

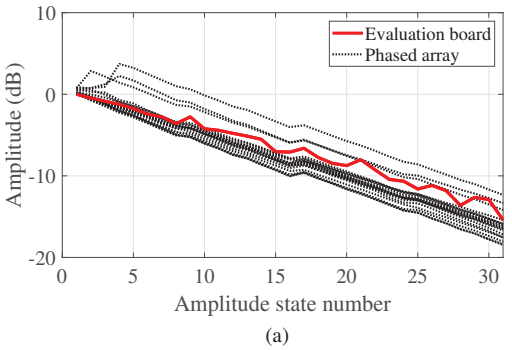

(a)

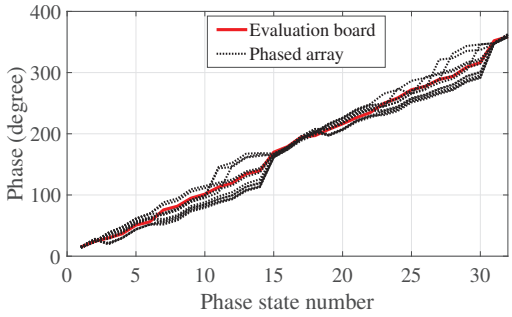

(b)

Fig. 5. Relative response of different elements versus the digital states: (a) amplitude and (b) phase.

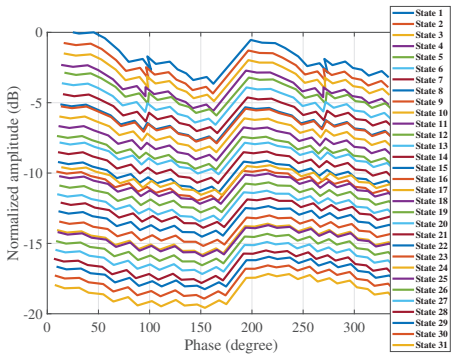

Fig. 6. Amplitude variations at each amplitude state of the VGA versus phase.

2 to 7 dB. Similarly, Fig. 5b shows the relative phase response of the MMIC channels with respect to phase state numbers while the VGA is at state 1. Like amplitude responses, phase responses are also different from each other and eval-board measurement data. The total phase variations over different MMICs varies between 0 to 60 degrees at different states.

Another issue with MMIC characterization is that the control of amplitude and phase are not completely independent. For example, as shown in Fig. 6, phase variations change the amplitude set by VGA. Fig. 6 shows 2 to 3 dB amplitude variations at each amplitude state as the phase changes. The phase variations over phase states versus amplitude changes are small. It is approximately 10 to 12 degree which is almost the same as the quantization error (~ 11.25 degrees).

To characterize the MMIC channels with independent VGA and phase shifter response, each of them are characterized independently. However, when the phase shifter and VGA are not completely independent, to fully characterize the MMIC channel of each antenna, every possible combination of phase and amplitude states of MMICs should be measured.

IV. Calibration Algorithm and Measurement Results

For the calibration of the system a near-field probe is periodically positioned in front of each radiating element while other elements on the array are deactivated. In the first step, we use the same initial settings for all the phase shifter and the VGA states. Then each element is activated individually to measure phase and amplitude offsets between all elements in the array as shown in Fig. 2.

The second step is to find the correct VGA and phase shifter states to apply the necessary corrections to realize uniform phase and amplitude distribution over the aperture.

One way to do that is to use the MMIC datasheet or eval-board measured characteristics data. It is a fast and simple way to find the correct command settings to compensate for the amplitude and phase unbalances of each element. However, as discussed in Section III, since the behaviour of the MMICs inside the array are different from those in eval-board, this simple method is not accurate enough. As shown in Fig. 3, the eval-board data can differ from real response of the MMIC inside the array by as much as 5 dB in amplitude and 40 degrees in phase.

The more accurate method is to first characterize each MMIC channel inside the array individually by measuring the relative change in amplitude and phase states for all digital settings and then to search for the proper state settings which compensate for all channel phase/amplitude unbalances. Since the phase shifter and VGA are not completely independent, ideally 32×32 measurements are required (instead of $32+32$) to fully and accurately characterize each channel of the MMIC. Considering the large number of elements (here 1024), it is a very time consuming process. Instead, we can use the eval-board data as the initial estimate and then apply an iterative search algorithm combined with measurement to obtain the results nearly as accurate as the exhaustive search. This fast search algorithm reduces the number of measurements from 992 to less than 15 numbers for each MMIC channel.

Fig. 7 shows the phase and amplitude variations of elements before and after calibration. The amplitude and phase variation before calibration is approximately 10 dB and 80 degree respectively. After the calibration and applying amplitude and phase offset corrections, the amplitude and phase variations are reduces to $\sim$ 3 dB (except for a few outlier points) and 15 degrees respectively. The error in phase is mainly due to quantization error ($\sim$ 11.25). The error in amplitude comes from the fact that it is not always possible to find a set of amplitude and phase states that satisfy the calibration criteria simultaneously. This comes from hardware non-idealities including quantization errors, limited dynamic range of VGA and dependency of the phase and amplitude.

The planar near-field (PNF) measurement system from NSI is used to measure the radiation pattern for different beam

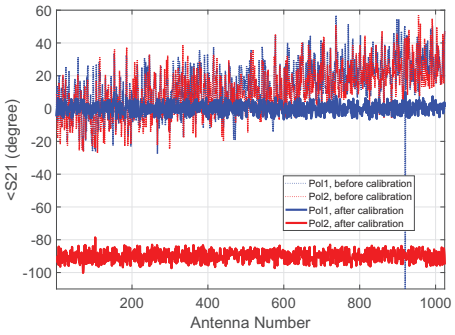

(a)

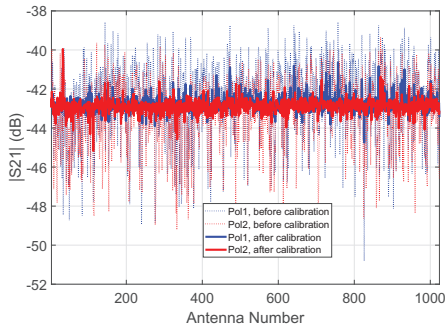

(b)

Fig. 7. (a) Phase and (b) amplitude of S21 for each element before (dotted lines) and after (solid lines) calibration. Each element has two polarization (two colors).

steering angles (Fig. 8a) and at different frequencies (Fig. 8b). Fig. 8a shows that the antennas radiation beam can be steered up to 70 degrees off-boresight. However, the gain of the array drops by the factor of $\cos(\theta_s)$ (θ_s is the scanning angle) and the side lobe levels are increased by steering the beam toward larger beam scan angles. Fig. 9 shows the normalized LHCP and RHCP broadside pattern at 19.5 GHz. The pattern is almost symmetric at boresight in both orthogonal planes. The cross polarization level of -25 dB is achieved.

V. Conclusion

In this paper the challenges of characterization and calibration of large scale modular active phased array antenna are discussed. Considering these challenges a very accurate and efficient calibration technique is suggested and verified successfully on K-band modular Rx phased array antenna with 1024 elements over a wide range of scan angles ($0-70$ degree) and wide frequency band of $18-21$ GHz.

Acknowledgement

The authors would like to thank Ontario Centres of Excellence (OCE), National Science and Engineering Research Council (NSERC) of Canada, and C-COM Satellite Systems Inc. for their financial supports

References

[1] H. Fenech, S. Amos, A. Tomatis, and V. Soumpholphakdy, "High throughput satellite systems: An analytical approach," *IEEE Transactions on Aerospace and Electronic Systems*, vol. 51, no. 1, pp. 192–202, January 2015.

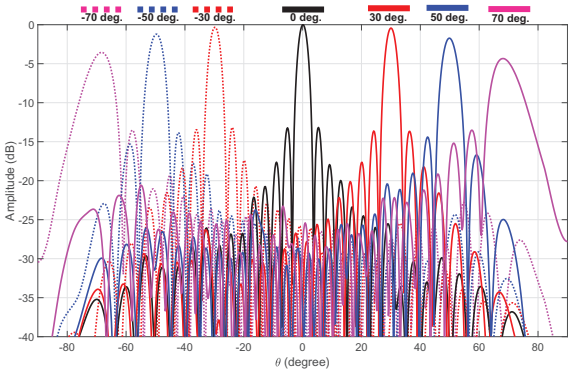

(a)

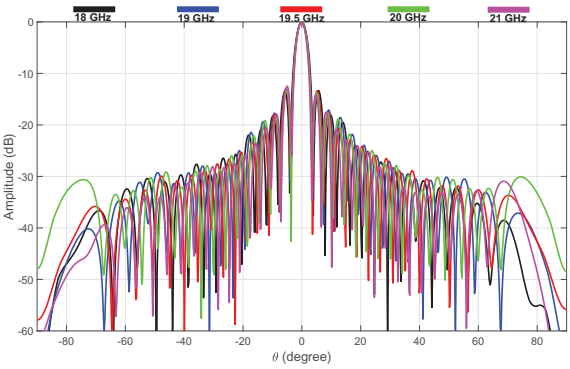

(b)

Fig. 8. (a) Measured normalized radiation pattern (LHCP) of 1024 element APAA for different beam steering angles at 19.5 GHz. (b) Measured normalized LHCP broadside pattern at different frequencies.

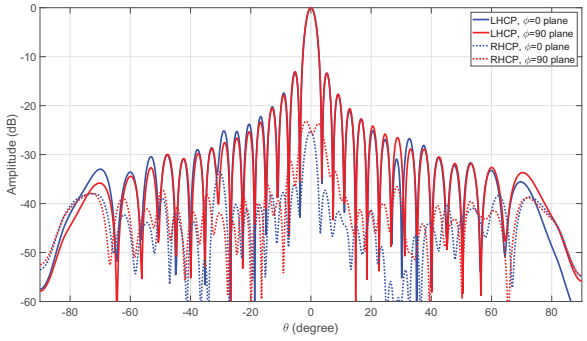

Fig. 9. Measured normalized LHCP (solid line) and RHCP (dotted lines) broadside patterns at 19.5 GHz in $\phi = 0$ (red curves) and $\phi = 90°$ planes.

[2] N. Saponjic, F. Klefenz, F. Bongard, D. Llorens, A. Boulle, X. Aubry, A. Butler, F. Tiezzi, and S. Vaccaro, "Product concepts for land mobile satellite communication terminals in Ku-/Ka-band," in *2017 11th European Conference on Antennas and Propagation (EUCAP)*, March 2017, pp. 1525–1529.

[3] P. Chiavacci, "The influence of phased-array antenna systems on LEO satellite constellations," *Microwave Journal*, pp. 282+, May 1999.

[4] W. M. Abdel-Wahab, H. Al-Saedi, E. H. Mirza Alian, M. Raeis-Zadeh, A. Ehsandar, A. Palizban, N. Ghafarian, G. Chen, H. Gharaee, M. R. Nezhad-Ahmadi, and S. Safavi Naeini, "A Modular Architecture for Wide Scan Angle Phased Array Antenna for K/Ka Mobile SATCOM," in *2019 IEEE MTT-S International Microwave Symposium (IMS)*, June 2019, pp. 1076–1079.